Signatures of Collective Local and Nanoscale Distortions in Diffraction Experiments

Angel J. Garcia-Adeva,*,† Dylan R. Conradson,† Phillip Villella,†,‡ and Steven D. Conradson†

Materials Science and Technology Division (MST-8), Mailstop G755, Los Alamos National Laboratory, Los Alamos, New Mexico 87545, and Department of Physics, University of Colorado, Boulder, Colorado 80309

Received: January 3, 2003; In Final Form: April 15, 2003

The effects of periodic and aperiodic distortions on the structure factor and radial distribution function of single-component lattices are investigated. To this end, different kinds of distortions are applied to the otherwise perfect square lattice and the corresponding radial distribution function and structure factor for the resulting lattices are calculated. When the applied distortions have a periodic character, they are very easily recognized in the calculated structure factors as new superlattice peaks. However, when the periodicity of the distortions is suppressed, the signatures of disorder only show up as smooth and subtle features on the diffuse part of the scattering, making it very difficult to identify the nature of the distortions present in the lattice. The implications of these results are discussed.

I. Introduction

Diffraction by X-rays (XRD) in the laboratory and at synchrotron facilities and neutrons at special sources are some of the most venerable experimental methods in physics, having made a prominent contribution in establishing many basic concepts in atomic and solid state physics. In particular, our understanding of XRD is so profound that it is routinely used for obtaining structural information about crystalline solids. In conjunction with very powerful structural analysis algorithms, it is a matter of hours to identify the crystallographic positions of the atoms of an unknown crystalline material. However, diffraction analysis relies on the well-founded paradigm of crystalline solids as the periodic repetition of a small pattern of atoms (the unit cell). Even though this description of solids can be considered as one of the pillars in the construction of the modern condensed matter physics, it is also true that the vast majority of real solids exhibit one or another form of structural disorder. Aperiodic disorder manifests itself in the structure factor as diffuse scattering.[1,2] Although it is possible to extract information from the diffuse part of the scattering, the analysis is complicated and relies strongly on the particular structural model chosen. The possibility therefore exists for uniqueness problems that make it very difficult to gain reliable information about the disorder present in real solids. Thus, conventional crystallographic analysis of diffraction patterns provides an excellent description of the average long-range arrangements of the coherent fraction of the atoms, without providing definitive or even incisive information about local distortions that may be coupled to the compelling properties of many complex materials. With the advent of local structure probes, however, lattice distortions are now recognized as an intrinsic characteristic of many correlated and transformational crystalline solids.[3,4] These include cuprate superconductors, manganite CMR compounds, martensities, and many alloys and other solid solutions.[5−11]

Two issues fundamental to lattice distortions are how are they organized and how are they best probed? Although seemingly disparate, these questions are actually closely associated. Close to 100 years of successful theoretical development and experimental application of crystallography make it appealing to many to assume that these distortions collectively exhibit a periodic component or are best understood as patterned deviations from the average symmetry. If this is the case, then high dynamic range momentum-space analysis of satellites and diffuse scattering associated with Bragg peaks would be the most accurate approach.[12−14] Alternatively, real space analysis of PDF and XAFS data would be advantageous if the lattice distortions under inspection are not correlated with the long-range average structure given by conventional crystallographic methodology.[15−17] One obstacle to the widespread acceptance of this view is that, having removed crystallography as the underlying basis for determining the arrangements of atoms, local structure proponents have no replacement by which local structure data can be extrapolated to construct the spatial relationships of the atoms in a material.

Inversely, although only rarely acknowledged, it is nevertheless obvious that the selected method strongly biases the result. Those who utilize momentum space find the periodicity that is inherent to their techniques, whereas real space practitioners do not. In the absence of a direct probe of bulk (as opposed to surface) structure on the nanoscale, it is difficult to demonstrate that reality most likely lies somewhere between, or actually includes, these two extremes. Even while both camps agree that all of the information required to construct the structure resides in the scattering data, the question of the best means for extracting it has become almost a religious debate.

The question of their organizing principles has become increasingly important with the realization that lattice distortions, via propagation and overlap of their local strain fields, may actually encompass an entire crystal even at quite modest levels of alloy/impurity element substitution. Diffraction data may point to a unit cell extended into a lattice, on which not a single atom actually resides even while it is defined by their spatial average.

Even more heretical is the natural extension of the idea that alloy/impurity elements or charge localization are the origin for the distortion. If directly bonded clusters are favored over a more

* To whom correspondence should be addressed.
† Los Alamos National Laboratory.
‡ University of Colorado.

10.1021/jp034016y CCC: $25.00
Published on Web 06/24/2003

dispersed distribution then macroscopic phase separation will result and the added elements will be insoluble. If these "defects" repel then they will tend to order into a periodic superstructure that may be associated with the host lattice or incommensurate. However, if they are randomly located or attract at distances farther than that for direct bonding, then the nanoscale domains exhibiting the larger fluctuations away from the average composition may tend to adopt a structure different from the bulk that is more compatible with their actual local stoichiometry. The size and morphology of these domains will be constrained by epitaxial forces at the interfaces with the bulk structure and may be filamentary rather than globular. Electronic as well as elastic forces may be important. If the disruption of the host electronic structure by a few atom percent of a trace element is part of the reason it may stabilize a particular phase, then if this perturbation can be thought of as a field, its magnitude will decrease with distance. Sets of atoms with low local concentrations of the stabilizing element may then tend to revert to the structure of the pure material. The net effect of this competition between local and global constraints will be the appearance of aperiodic phase separation in the mesoscale, the effects of which in the diffraction patterns are simply not known.

It may thus seem surprising that, despite the abundant examples in the literature that try to stress the importance of the aforementioned scenario,[18−30] the properties of complex systems are oftentimes analyzed based on information extracted from conventional structural analysis (i.e., Bragg refinement) which, in most cases for these systems, provides a picture of their microscopic structure which is, simply put, wrong. One possible reason for this is that accepting this picture of complex solids in terms of organizing principles acting on very different length scales would make things extremely complicated. Therefore, it is easier to rely on a "well-established" description of solids rather than implementing an expensive and difficult program based of the previous facts. It is for this reason that we think that it is especially important to draw the attention of researchers toward the fact that taking an unilateral approach based on conventional structural analysis can lead to ignoring effects such as nanoscale heterogeneity or aperiodic phase separation which are, obviously, essential in understanding the physical properties of complex materials. This is precisely the purpose of the present work. We report the results of simulations of the structure factors and radial distribution functions (RDF) in lattices with different kinds of isolated and collective distortions. For simplicity, we have carried on the calculations in two-dimensional lattices. However, the conclusions drawn in this work are extensible to real three-dimensional lattices . We will show that ignoring apparently small and unimportant features usually present in the diffuse scattering can lead us to develop models and extract conclusions from these models for systems that, simply put, have nothing to do with the real solid under consideration. Moreover, we will also show that, even in some extreme cases, aperiodic distortions affecting one-fifth or more of the atoms in the lattice can barely affect the calculated structure factors when compared with their periodic counterparts, making it very easy to miss them by using conventional analysis methods. We will also see that even in some cases, where distinct features of disorder are present, we can easily devise different types of distorted configurations that lead to qualitatively similar structure factors, making it very difficult to ascertain the nature of the underlying lattice. Our primary motivation for performing these calculations is our local structure measurements that show cooperative effects between solute atoms in several alloys and oxides that apparently culminate in up to 20−25% of the atoms being involved in a structure that is differently ordered than the bulk, crystallographic phase in some of these materials.[3,21,26] These experiments point to the presence of what we have termed nanoscale heterogeneity, in which nanoscale domains that are intimately associated with the bulk material adopt a (radically) different but still ordered arrangement of their constituent atoms, perhaps resulting from natural and/or induced composition fluctuations on this same length scale. A serious problem in gaining credibility for this interpretation is the lack of a signature for these second structures in diffraction measurements, since they should be sensitive to the presence of an additional phase at this level. Therefore, it is very important to assess if and how one out of four/five atoms could be present in a second structure without diffracting.

The remainder of this paper is organized as follows. In the next section, we will describe the lattices we have considered in this work. In section III, the results of our calculations for the RDF and structure factors, and a discussion of the main results are presented. Finally, section IV is devoted to stating the conclusions of this work.

II. The Distorted Lattices

As briefly mentioned in the Introduction, we have considered 2D square lattices to which different kinds of static disorder have been applied in order to simulate various possible lattice distortions. For completeness, we have also considered purely periodic lattices obtained by distorting the square lattice (see below). The size of all of the lattices reported in this work is 40×40 atoms (1600 atoms). This is a compromise between large enough lattices so the finite size effects are small while, at the same time, keeping the CPU time down to a reasonable amount (hours). Obviously, the finite size of the lattices will give rise to a broadening of the peaks in the calculated structure factors that makes it difficult to extract any conclusion about how these distortions affect the shape of the diffraction peaks. However, such an analysis of the shape of the peaks is outside the scope of this work and, besides, based on comparisons with the results for smaller lattices, this broadening does not modify any of the conclusions reached in this work about the effects of distortions on the diffuse scattering. A more rigorous proof of this statement will be given below. The lattice parameter used in all of the calculations is 3 Å. Let us now briefly review the different kinds of distortions that have been applied to the otherwise perfect square lattice:

Vacancies. The first case we have considered consists of different configurations of vacancies placed on the square lattice (see Figure 1). The first and simplest configuration of vacancies consists of randomly removing 20% of the atoms of the lattice in order to test the effect of random, aperiodic elimination. In addition, we have also considered configurations in which the positions of the vacancies are not random, but correlated, forming channels across the lattice and periodic and aperiodic distributions of vacancies defining certain regular geometric shapes. Finally, we have also considered a configuration in which the vacancies define different regular shapes which are randomly placed in the lattice.

Atoms Displaced from Their Original Crystallographic Positions (Figure 2). The configurations considered in this case are similar to the previous ones. The first type of displacements we have considered consists of randomly choosing 20% of the atoms of the lattice and displacing them by a vector ($\cos\theta$, $\sin\theta$), where θ randomly varies among 32°, 148°, 212°, and 328°

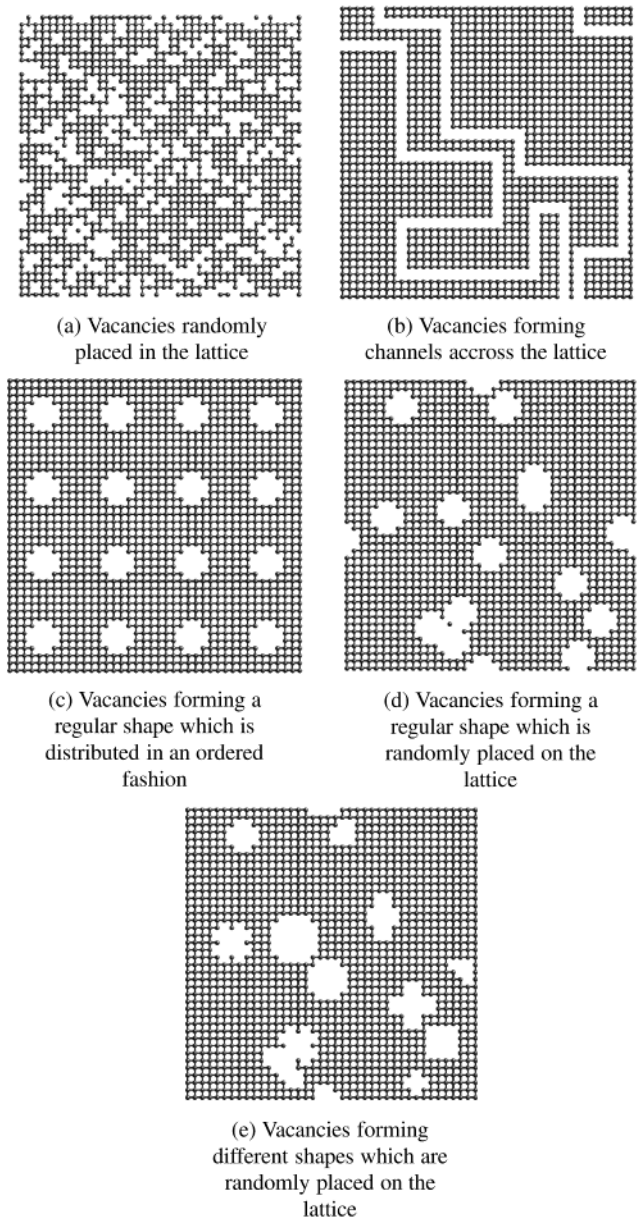

Figure 1. Configurations of vacancies considered in this work.

(see Figure 2a). The second type of displacements we have considered is similar to the channel of vacancies explained above, except for the fact that now, instead of removing the atoms, they are displaced by the same random vector as in the previous displaced configuration (see Figure 2b). We have also considered the case in which a certain number of atoms defining a regular shape (a small cross) are displaced by the same random vector, and this shape is periodically and aperiodically repeated across the lattice (see Figure 2, parts c and d). Finally, we have also tested the effect of having two phases of different symmetries inside the lattice. To this end, the interatomic distances between the atoms defining the crosses used in the last two configurations have been contracted by a factor 0.04*a* in the horizontal direction. These two configurations have not been depicted, at the visual differences with respect to the last two cases are barely noticeable.

Inclusion of a Tetragonal Domain. We have considered the effect of contracting a regular domain (a square domain) in the horizontal direction by an amount 0.04*a* (see Figure 3). To see what is the minimum size this domain has to be in order to

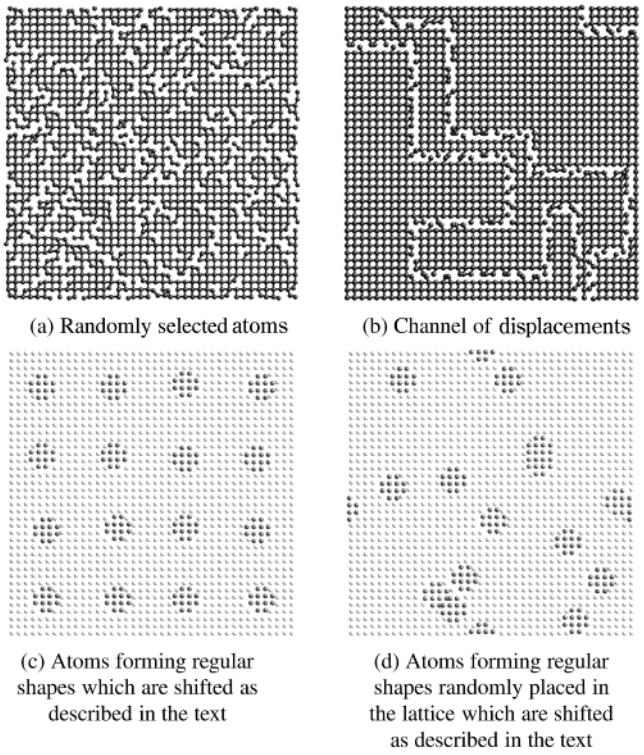

Figure 2. Lattices with atoms displaced from their crystallographic positions. As explained in the text, we have also considered two additional cases not depicted here, analogous to cases c and d, where the small crosses are additionally contracted an amount 0.04*a* in the horizontal direction.

show up in the $S(Q)$, different domain sizes have been considered, ranging from 4×4 atoms up to 40×20 atoms (half the lattice is contracted). Additionally, we have also considered a lattice in which the positions of groups of atoms defining a geometric motif (a small cross), randomly placed in the lattice, have been tetragonally distorted (see Figure 3b).

Periodic and Aperiodic Modulated Distortions (Figure 4). Each of the elementary square cells in the lattice is assigned a position vector of the form (i, j), where i and j are both integer numbers. For example, the (1,0) cell would correspond to the cell defined by the atoms located at (0,0), (0,*a*), (*a*,0), and (*a*,*a*). To implement this kind of distortion, in the periodic case, the positions of all the atoms on the corners of the cells with odd i and j have been shifted toward the center of the corresponding cell by a 4% of the undistorted lattice parameter (see Figure 4a for details). The resulting lattice can be seen as another square lattice of lattice parameter 2*a* with a basis. In the aperiodic case (Figure 4b), the procedure is similar to the periodic case, but we have allowed the direction of the contraction to randomly vary among the values 25°, 45°, and 65°.

Periodic and Aperiodic Interstitial Atoms. Using the periodic modulated lattice described in the previous paragraph, an interstitial atom has been placed inside each of the squares defined by those atoms with largest bond length (see Figure 5). In the periodic case, the interstitial atom is located in the center of the square. Again, this new lattice can be seen as a square lattice of lattice parameter 2*a* with a basis. In the aperiodic case, the interstitial atom is randomly located in a circle of radius 0.04*a* centered at the middle point of the square (see Figure 5b for details).

Periodic and Aperiodic Channels of Defects across the Lattice. In this case, the effect of correlated networks of defects has been studied. In the periodic case, all of the atoms belonging

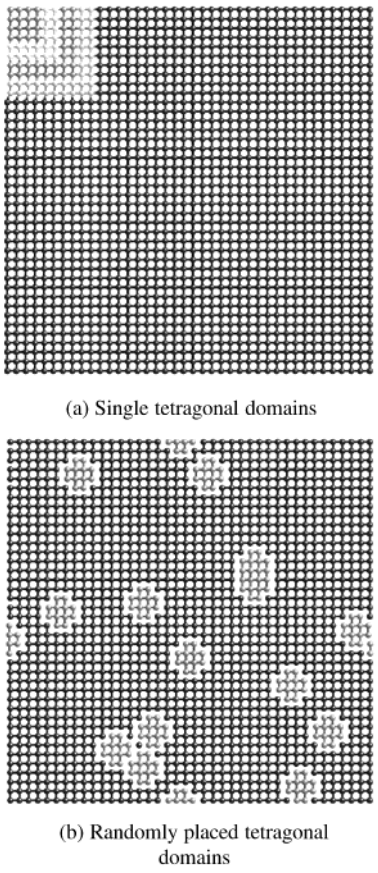

(a) Single tetragonal domains

(b) Randomly placed tetragonal domains

Figure 3. Inclusion of tetragonally distorted domains in the square lattice. In a, we have shaded with different grays some of the domains considered in this work, in particular, 4×4, 6×6, 8×8, and 10×10 atom domains. In b, the interatomic distances of the atoms belonging to the small crosses are contracted by an amount 0.04a.

to a chosen column have been shifted downward by half the lattice parameter. At the same time, the atoms belonging to this channel have been shifted in the horizontal direction by an amount of $+a/6$ or $-a/6$, respectively (see Figure 6a). In addition, each seventh atom in the network has been removed. Finally, the distorted network has been periodically repeated across the horizontal direction. In the aperiodic case, channels across the lattice similar to the ones introduced in the case of vacancies and displacements have been considered (see Figure 6b). However, in contrast with the displacements case, the atoms inside this channel have been alternatively displaced horizontally or vertically, in such a way that they define a second tetragonal phase inside the square lattice, whereas in the displacements case, the displacements where applied in a random fashion. Moreover, each seventh atom has been removed.

As stated in the Introduction, our intention is to study how these different types of distortions affect the calculated diffraction patterns. The result of this analysis is presented in the next section.

III. Results and Discussion of the Calculated Structure Factors and Radial Distribution Functions

The static structure factor (SF) $S(Q)$ and radial distribution function (RDF) $g(r)$ have been calculated for the lattices introduced in the previous section. To this end, we have used the code CRYGEN2D, developed by P. Villella and co-workers at Los Alamos National Lab.[31] This program takes as input the coordinates of the atoms in a two-dimensional lattice and exactly computes the RDF and $S(Q)$. The RDF is defined as the

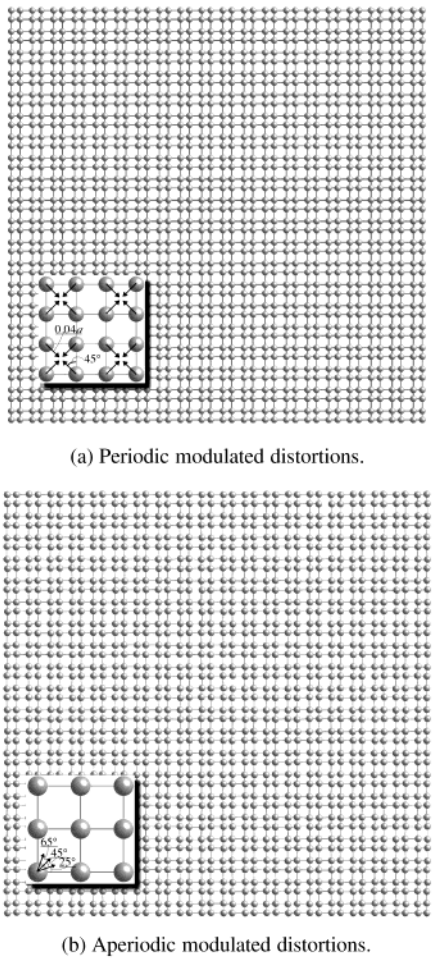

(a) Periodic modulated distortions.

(b) Aperiodic modulated distortions.

Figure 4. Modulated lattices. The insets show how the distortions are implemented in both the periodic and aperiodic cases.

spherical average of the pair distribution function[32]

$$G(\vec{r}) = \frac{1}{N}\sum_{i\neq j}\langle\delta(\vec{r} - (\vec{r}_i - \vec{r}_j))\rangle \qquad (1)$$

where N stands for the number of atoms in the lattice and $\langle ... \rangle$ represents a thermal average. In practice, $g(r)$ is calculated for finite size lattices by taking each atom in turn as the origin and calculating the number of atoms located between r and $r + \Delta r$, where Δr is a small number (typically 0.001 Å in our calculations). In two dimensions, this function is related to the coordination number z in a ring from $r_{\min}$ to $r_{\max}$ by the expression

$$z = 2\pi \int_{r_{\min}}^{r_{\max}} g(r) r \, dr \qquad (2)$$

To normalize the results reported below, each calculated $g(r)$, for a particular lattice, has been divided by the area under the curve. This normalization choice makes it easier to compare relative changes in the intensity of the peaks for the various lattices considered in this work. The SF is calculated in reciprocal space by using the standard definition[2]

$$S(\vec{Q}) = \frac{1}{N}\sum_{i,j} f_i(\vec{Q})\, f_j(\vec{Q})\, \langle e^{i\vec{Q}\cdot(\vec{r}_i - \vec{r}_j)}\rangle \qquad (3)$$

where f_i are the atomic form factors and an average over the angular degrees of freedom is performed in order to calculate

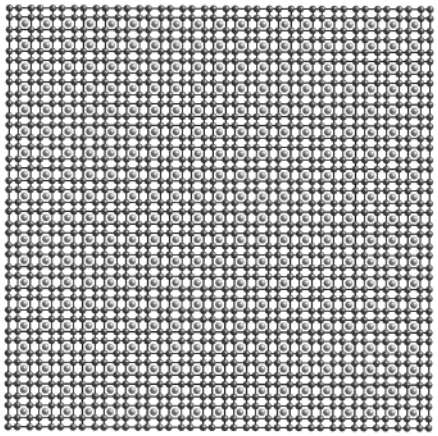

(a) Periodically distributed interstitial atoms

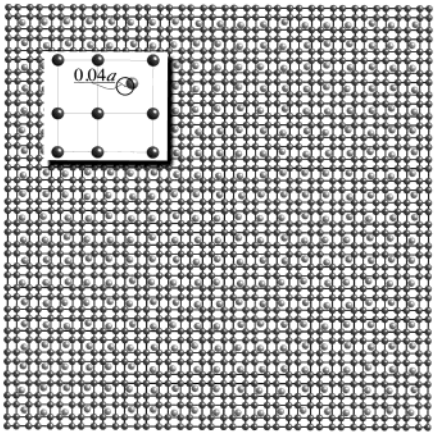

(b) Aperiodically distributed interstitial atoms

Figure 5. Lattices with interstitial atoms. The inset in part b shows how the interstitial atoms are placed on the lattice in the aperiodic case. They are placed on a randomly chosen point of the circumference with center at the center of the cell and radius 0.04*a*.

the powder pattern. The thermal average contains the effects of thermal motions of the atoms at finite temperature. In the simplest approximation (Debye approximation), it is assumed that all of the atoms are subject to small uncorrelated vibrations at the same frequency. In this limit, the thermal average can be performed analytically giving rise to a modified expression for the SF of single-component lattices

$$S(\vec{Q}) = f(\vec{Q})^2(1 - e^{-2M}) + \frac{1}{N} f(\vec{Q})^2 e^{-2M} \sum_{i \neq j} e^{i\vec{Q}\cdot(\vec{r}_i - \vec{r}_j)} \quad (4)$$

where e^{-2M} is the temperature factor with $2M \sim Q^n$ (n depends on the dimensionality of the lattice, for example, $n = 2$ in three dimensions) the Debye−Waller factor and the $\vec{r}_i$ are now the static positions of the atoms without the thermal displacement part. The effect of the thermal factor is 2-fold. On one hand, the intensity of the Bragg peaks is attenuated, with this attenuation being stronger at larger values of Q. On the other hand, it gives rise to a continuous diffuse background (thermal diffuse scattering) that increases as Q increases. Devising theoretical models for the effects of correlated thermal motions on the thermal diffuse scattering is a highly nontrivial problem and still constitutes an active field of research.

In the calculations reported below, the thermal diffuse scattering at finite temperature has been simulated by allowing small random deviations of the atomic positions with regards to their equilibrium positions. The maximum allowed amplitude for these deviations is 0.05 Å, and they are distributed according to a Gaussian normal distribution. In this sense, no approximation is made in this calculation apart from the finite size of the lattices.

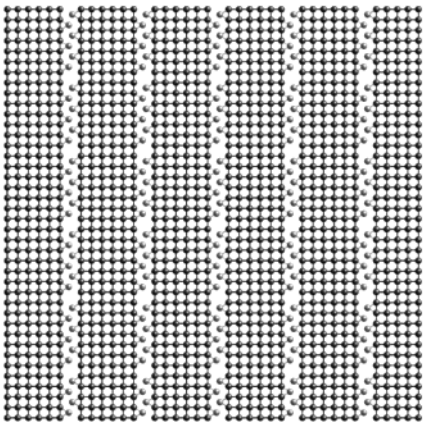

(a) Periodic channels

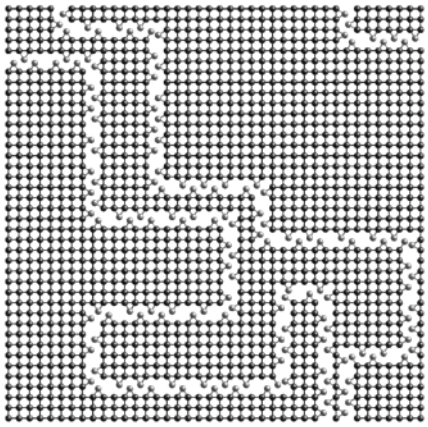

(b) Aperiodic channels

Figure 6. Lattices with channels of tetragonal distortions.

For comparison, the $S(Q)$ and $g(r)$ of a 40×40 atoms square lattice have been also calculated and used as reference. The $S(Q)$ data have been normalized in order to eliminate differences coming from the different number of atoms present in some lattices with respect to the square one. This allows us to compute the difference between any two $S(Q)$ data sets, so the differences in the diffuse scattering are more noticeable. The results of the $S(Q)$ calculations are presented below in terms of the dimensionless variable $(Qa/2\pi)^2 = h^2 + k^2$ (with h and k the Miller indices), which makes it very simple to assign the Bragg peaks. Let us now review how these different kinds of distortions affect the calculated $g(r)$ and $S(Q)$.

Effect of Random Vacancies. The results for the RDF and $S(Q)$ can be seen in Figure 7. As one would expect, the only effect of vacancies on the RDF is a reduction in the intensity of the peaks proportional to the concentration of vacancies in the lattice.

The situation is a little more complicated for the calculated structure factors. The fundamental peaks are located at the same positions as for the square lattice and have the same shapes. Their intensities, however, are smaller for the lattices with vacancies than for the square lattice because part of the intensity goes now to the diffuse part of the scattering. For the case of 20% atoms randomly removed from the lattice, the main effect is an increment of the background, very similar to the effect of

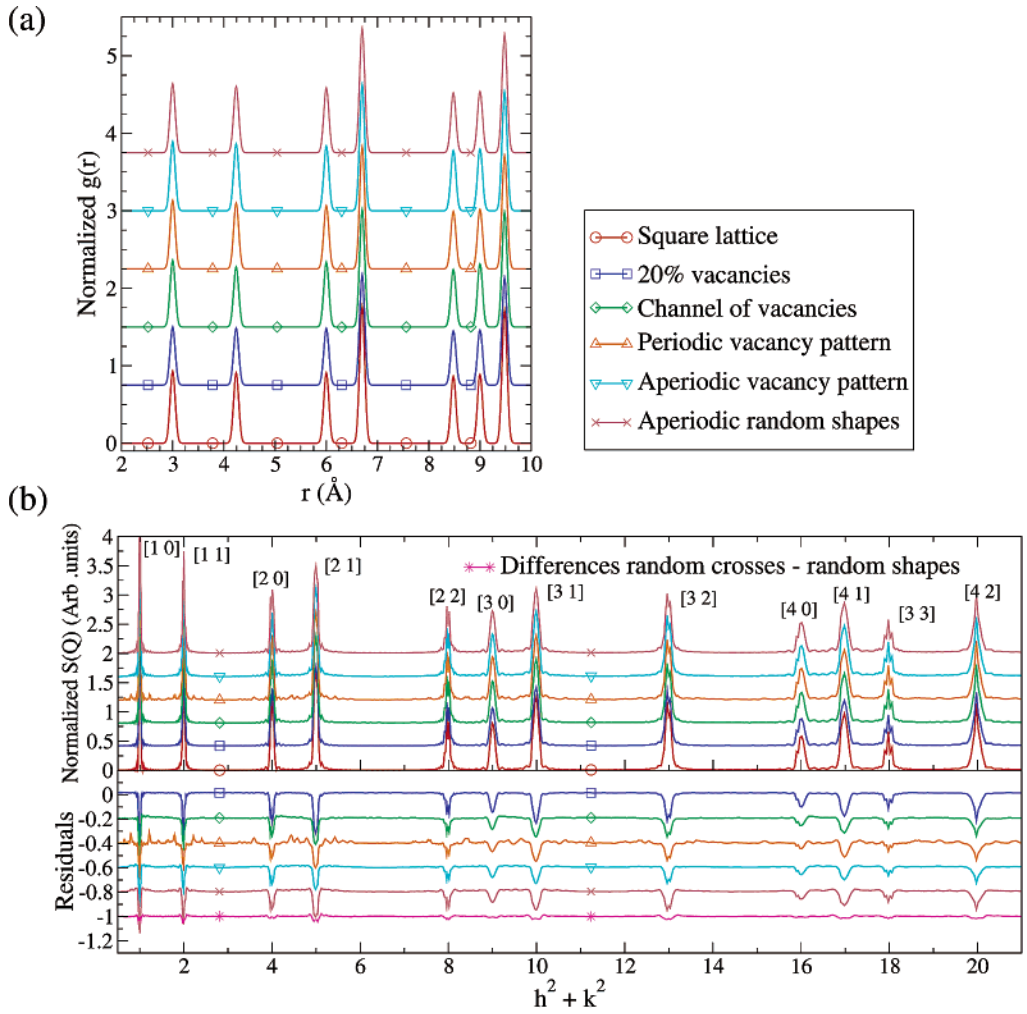

Figure 7. (a) RDF and (b) $S(Q)$ for the lattices with vacancies. The assignments of the diffraction peaks of the square lattice are shown in the upper panel of b for reference. The lower panel shows in greater detail the difference between the $S(Q)$ of the square lattice and the ones of the distorted lattices. To construct these curves, the $S(Q)$ have been properly normalized and the $S(Q)$ of the square lattice has been subtracted from the rest of $S(Q)$ of the distorted lattices. The units used in that panel are the same as the ones used in the upper panel. In this way, negative values correspond to regions in which the $S(Q)$ of the square lattice is larger than the corresponding one for the distorted lattice. As expected, peaks with negative values occur at the positions of the fundamental peaks of the square lattice diffraction pattern, whereas peaks with positive values correspond to additional features coming from the distorted character of the lattices (superlattice peaks or diffuse scattering). The green curve labeled "Differences random..." has been obtained by subtracting the $S(Q)$ of the lattice in Figure 1e from the one of the lattice depicted in Figure 1d.

a Debye−Waller factor, except for the fact that this background is essentially constant for all Q's, in contrast to the Debye−Waller diffuse scattering, which is larger for larger values of Q. In the case of the channels of vacancies extending through the lattice, the main effect is an increment of the diffuse scattering around the [i 0] (i = 1, 2, 3, ...) peaks. This enhancement is highly asymmetric, affecting only the high-Q part of the peak.

If we now turn our attention to the configurations in which vacancies define geometric shapes, we can see that, in the periodic case, many new peaks appear at incommensurate positions with respect to the spacing of the original square lattice. Obviously, these new peaks are nothing but superlattice peaks associated with the fact that the lattice can still be seen as a square lattice of lattice parameter 10a with a complicated basis. We will further comment on these superlattice peaks below. In contrast, if these shapes are randomly distributed, the superlattice peaks disappear, and the background acquires a modulated character: there is an enhanced diffuse scattering around the fundamental peaks, and this background is depleted in between. The combination of these two effects give rise to some kind of oscillatory diffuse scattering. This effect is more noticeable at low Q. We wanted to check if these oscillations were due to the fact that all of the defects have the same size and shape, and to this end, we repeat this calculation using different shapes and sizes but located at the same positions (see Figure 1e). As can be seen from the green curve in the lower panel of Figure 7b, this is not the case, and the only difference between these two configurations is a barely noticeable increment of the diffuse scattering around the fundamental peaks at larger Q, in this last case.

Effect of Aperiodic Displacements. The results for this case can be seen in Figure 8. The RDF for the distorted lattices shows the original peaks of the square lattice (the intensity of these peaks is reduced, as expected) plus additional new peaks due to the new pairwise distances introduced by the displaced atoms. The new distances are especially apparent in the RDF for the lattice in which 20% of the atoms are randomly chosen and shifted from their crystallographic positions. For example, if we consider the peak corresponding to the nearest neighbor (NN) distances, we can see that four new peaks corresponding to the four new NN distances introduced by the distortions. The intensity of these new peaks are the same, as each of the four displacement vectors are equally probable. Similar comments

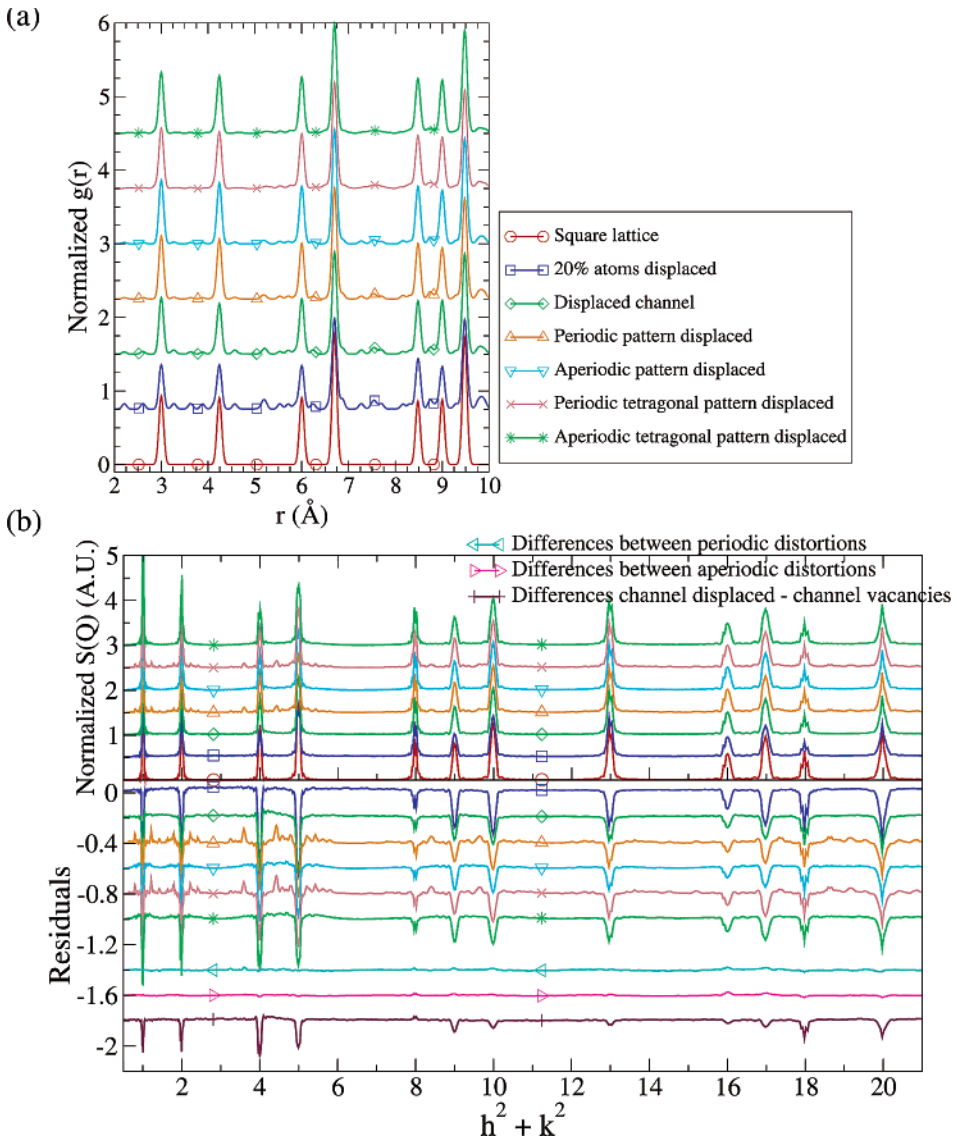

Figure 8. (a) RDF and (b) $S(Q)$ for the lattices with displacement distortions. See the comments in the caption of Figure 7 about how the lower panel has been constructed. The curve labeled "Differences between periodic distortions" has been calculated by subtracting the $S(Q)$ of the lattice depicted in Figure 2c to the one of the analogous lattices where additional tetragonal contractions have been applied to the small crosses distributed in an ordered fashion in the lattice. The same procedure has been applied to construct the brown curve in that panel but using the analogous lattices where the small geometrical motifs are randomly placed.

apply to further neighbor peaks. The other configurations exhibit exactly the same features as this last one: The same new peaks appear and they are located at the same positions. The main difference is the intensity of the new peaks which, obviously, is higher for those configurations involving a larger number of atoms displaced (320 atoms in the case of the 20% randomly chosen atoms to be compared with 200 in the channel case and 192 for the shifted crosses, respectively). This reduction in the intensity of the peaks is especially noticeable in those configurations in which the displaced atoms define a regular shape, as in this case the only new distances are located at the interface between the displaced and undistorted lattice. When additional tetragonal contractions are applied to these shapes, there are also new distances between the atoms defining the shape itself (for example, the NN distance in the horizontal direction is now 2.88 Å). However, these new distances are masked by the thermal broadening of the peaks associated with the regular part of the lattice.

The situation is more complicated for the calculated $S(Q)$. The intensity of the fundamental peaks decreases as part of it goes into additional structure appearing in the diffuse part of the scattering. For the configuration in which 20% of the atoms are randomly chosen and shifted, the background scattering exhibits modulated variations (enhanced background at low Q, depleted at intermediate values, and enhanced again at high values of Q), giving the impression of an oscillatory background, clearly different from the effect of purely thermal disorder. For the channel of displaced atoms, the behavior of the diffuse scattering is very similar to that of the channel of vacancies discussed above: The high-Q part of the [i 0] (i = 1, 2, 3, ...) reflections is enhanced. For comparison, we have depicted the difference between the $S(Q)$ for this configuration and the one for the channel of vacancies (the violet curve in the bottom panel of Figure 8b). As can be seen from that curve, the only difference between the $S(Q)$ for these two configurations is the intensity of the fundamental reflections. For other values of Q, this curve is essentially a flat line.

If we now turn our attention to the configurations where the shifted atoms define geometrical shapes, we can observe from Figure 8b that the results for those cases in which the regular

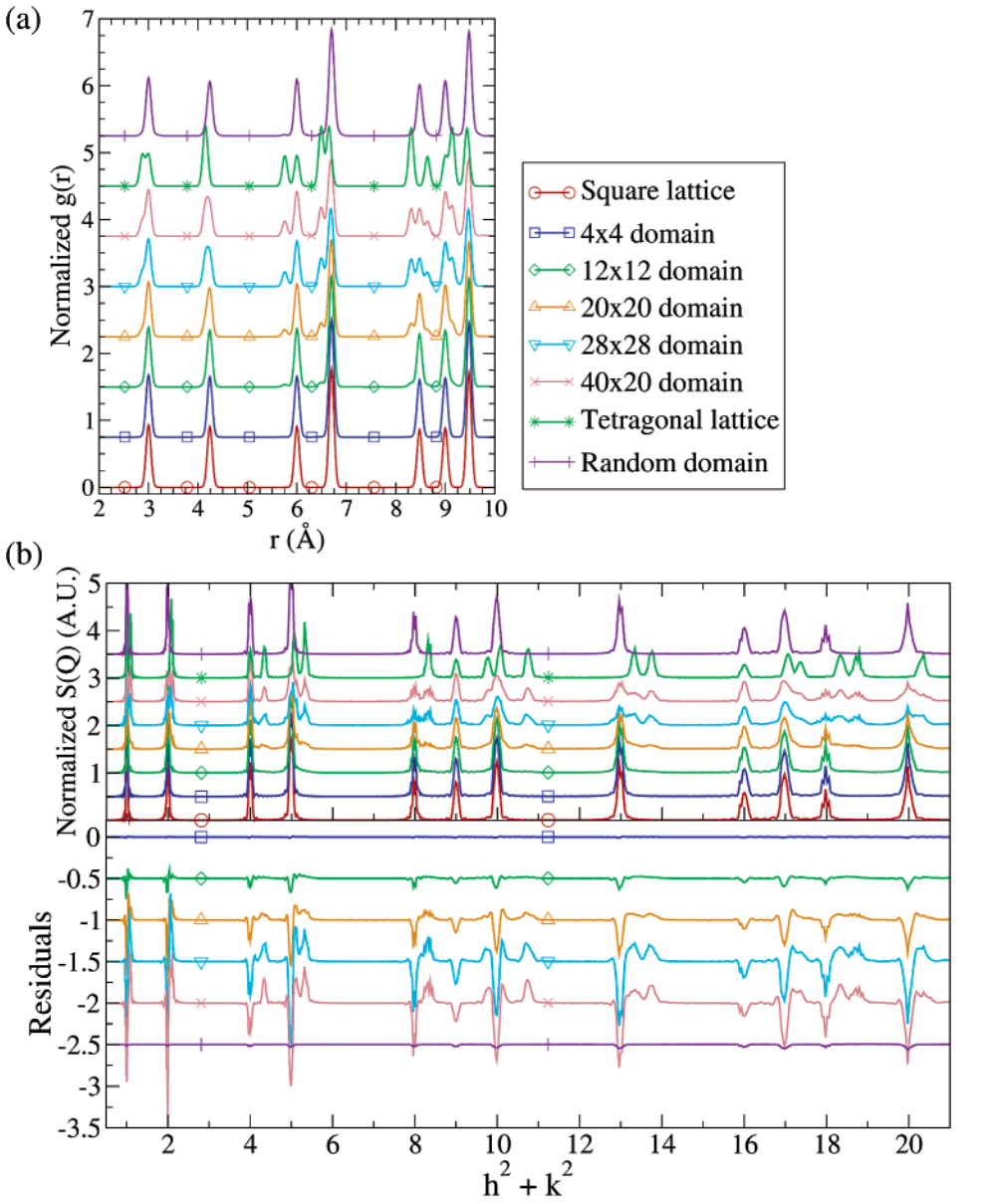

Figure 9. (a) RDF and (b) $S(Q)$ for the lattice with a tetragonal domain. See the comments in the caption of Figure 7 about how the lower panel has been constructed.

shapes are periodically chosen and then randomly shifted (both with and without tetragonal contraction) are very interesting: The resulting $S(Q)$ resembles that of a periodic lattice (appearance of superlattice peaks at incommensurate [h k] values), even though there does not exists an elementary motif (unit cell) from which the whole lattice can be obtained by periodic repetition. When these shapes are randomly distributed, the resulting diffuse scattering lacks any sharp features, and instead, it exhibits an oscillatory character with enhanced diffuse background around the fundamental reflections and depleted in between. Strikingly, the calculated SFs for both the regular shapes with and without tetragonal contractions are essentially identical, as can be seen from the green and brown curves in the bottom panel of Figure 8b, which are essentially flat lines. These observations imply that, even though we can induce the presence of a random or ordered motif of defects, it is difficult to judge whether this motif contains no atoms at all or a phase with a symmetry completely different from the one of the initial lattice. We will further develop this point when stating the conclusions of this work.

Effect of the Inclusion of a Tetragonal Domain. The results of the calculations for this type of distortions can be seen in Figure 9. In that figure, we have only depicted the results for some representative domain sizes. For the sake of comparison, the $S(Q)$ for a 40 $\times$ 40 lattice tetragonally contracted in the horizontal direction is also shown. As stated above, we also show in that figure the results RDF and $S(Q)$ for the lattice depicted in Figure 3b, where randomly placed regular shapes have been horizontally contracted. The RDF for those lattices with a single tetragonal domain nicely interpolates between the one for the square lattice and the one of a purely tetragonal lattice, and peaks associated to the new distances inside the tetragonal domain clearly develop as the domain size increases. It is interesting to note, though, that for practical purposes, below a domain size of 12 $\times$ 12 atoms, the new distances are barely noticeable in the RDF. The RDF for the randomly distributed tetragonally contracted shapes is very similar to the one consisting of a single tetragonal domain with the same number of atoms with the only difference of some small and broad peaks occurring at higher distances associated to the distances between

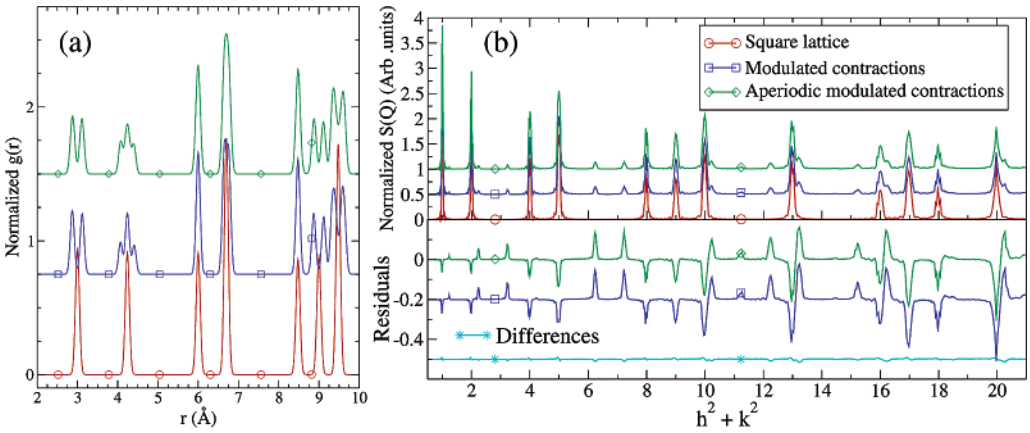

Figure 10. (a) RDF and (b) $S(Q)$ for the modulated lattices. See the comments in the caption of Figure 7 about how the lower panel has been constructed.

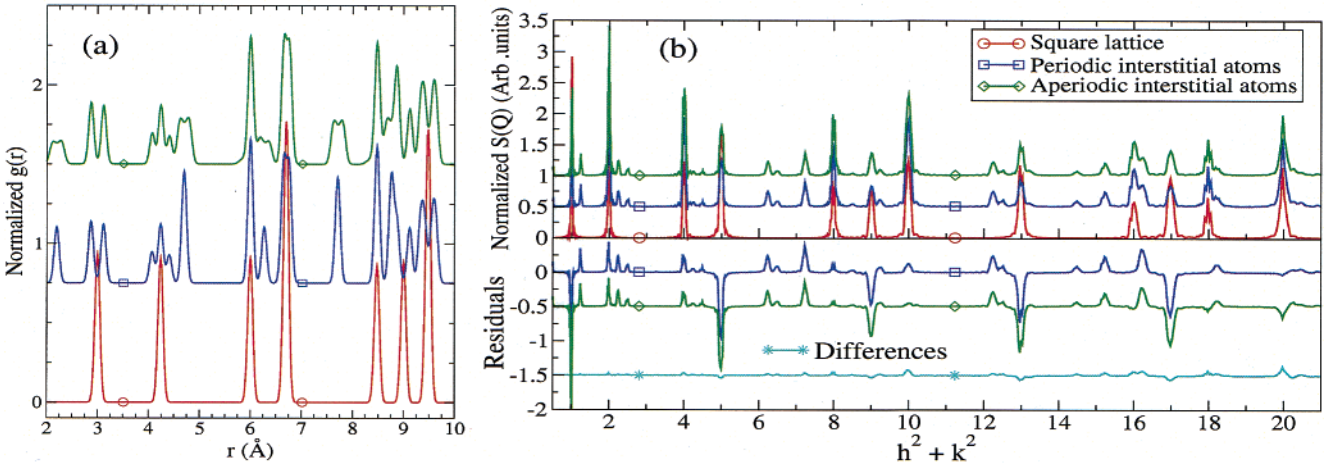

Figure 11. (a) RDF and (b) $S(Q)$ for the lattices with interstitial atoms. See the comments in the caption of Figure 7 about how the lower panel has been constructed.

the boundaries of the geometrical shapes and the atoms in the square phase.

Regarding the $S(Q)$, we can see in Figure 9b that new peaks, typical of the tetragonal symmetry, develop as the domain size is increased. Interestingly, these peaks are only noticeable for large domain size and, even for the 40 × 20 domain, the tetragonal peaks are not fully developed. However, the resulting $S(Q)$ for this lattice is fully consistent with the one obtained by adding up the $S(Q)$ for a square 40 × 20 lattice plus the one for a 40 × 20 one. Furthermore, the positions of the fundamental reflections are shifted to higher Q, because of an overall (though small) contraction of the lattice. Even though we have not shown it in that figure, we found that for sizes smaller than 12 × 12 atoms the new peaks are barely noticeable. The $S(Q)$ for the lattice with tetragonal shapes randomly distributed is essentially identical to the one of the square lattice, as can be seen in the lower panel of Figure 9b.

Effect of Periodic and Aperiodic Modulated Distortions. The results of the calculations for this type of distortions can be seen in Figure 10. The RDF for the modulated lattices (both periodic and aperiodic) are quite distinct from the square lattice one, as new distances are generated in the distorted lattices. As a result of these distortions, some of the peaks (noticeably the ones corresponding to NN, next NN, sixth NN, and seventh NN) are split reflecting these new distances, whereas in other cases (third, fourth, and fifth NN) the only effect is an additional (small) broadening superimposed to the thermal one. We can also see that the RDF for the aperiodic lattice is very similar to the periodic one, as we could expect from the fact that the distortions we have implemented average out to zero. The only noticeable difference is an slight additional broadening of the split peaks.

The $S(Q)$ for these lattices shows interesting features again. In the periodic case, many new small superlattice peaks at incommensurate h and k values appear associated with the fact that the modulated lattice is another square lattice of parameter $2a$ with a basis. The interesting point, however, is that the $S(Q)$ for the aperiodic modulated lattice is almost identical to the periodic one, as can be seen from the curve labeled "Differences" in the lower panel of Figure 10b. The only noticeable difference is the appearance of a marginal amount of diffuse scattering close to the fundamental reflections. Moreover, in both the periodic and aperiodic cases, the original peaks are only minimally affected until $h^2 + k^2 \approx 16$.

Effect of Periodic and Aperiodic Interstitial Atoms. The results of the calculations for these types of lattices can be seen in Figure 11. Regarding the RDF calculation, new distinct peaks appear associated with the new atom in the basis (see Figure 11a), when compared with the calculated RDF for modulated lattice described above. This is especially clear in the periodic case. In the aperiodic case, these same peaks remain, but they are broadened by disorder, as expected.

Regarding the results for the $S(Q)$, this quantity exhibits the peaks already described in the modulated lattice case plus new superlattice peaks associated with the sublattice of interstitial atoms. However, in full analogy with the previous case, the

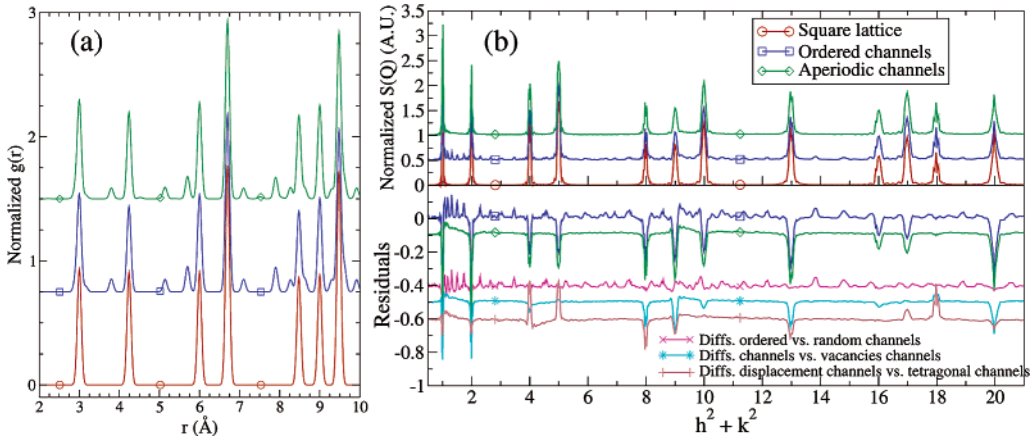

Figure 12. (a) RDF and (b) $S(Q)$ for the lattices with tetragonal distortions forming channels. See the comments in the caption of Figure 7 about how the lower panel has been constructed.

$S(Q)$ for the aperiodic case is essentially identical to the periodic one, the difference between these two cases being again a slight increment of the diffuse scattering around the fundamental peaks. When compared with the same curve for the modulated lattice, the only difference is that the differences in the diffuse scattering around the fundamental reflections slightly increased at higher Q.

Effect of Networks of Tetragonal Distortions across the Lattice. The results of the calculations for these lattices can be seen in Figure 12. The main effect of these distortions in the RDF is to produce many new peaks associated with the new pair distances inside the tetragonal channels. Interestingly, there are no noticeable differences between the periodic and aperiodic cases. This is not the case, however, for the $S(Q)$. The periodic channels give rise to new superlattice diffraction peaks as happened in all of the cases where the distortions were periodic. When the periodicity is removed, these superlattice peaks disappear and there is an enhancement of the diffuse scattering localized around the fundamental peaks of the square lattice, even though the RDFs for both lattices were essentially identical. It is interesting to notice that this enhancement of the diffuse scattering is somewhat similar to the one observed for the channel of vacancies and channel of random displacements. However, in this case, the enhancement only occurs at the high-Q part of the [i 0] reflections, with i an odd integer. For completeness, we have included the differences between the $S(Q)$ for the aperiodic channel of tetragonal distortions (Figure 6b) and the ones for the channel of vacancies (Figure 1b) and the channel of aperiodic displacements (Figure 2b) in the lower panel of Figure 12b. Apart from differences in the relative intensities of the fundamental peaks, the main difference occurs, obviously, around the high-Q part of the [i 0] reflections, for the reasons commented above. The rest of the diffuse scattering is essentially the same for the three lattices.

A. A Comment on the Superlattice Peaks. Throughout this work, we have consistently observed that the effect of periodic lattice distortions on the calculated structure factors is the appearance of localized peaks, with very small intensities, at incommensurate values of the Miller indices. We have denoted these peaks as superlattice peaks or superlattice reflections, extending the common usage of these terms that are usually used for nonstoichiometric compounds with chemical disorder[2] to the present monocomponent lattices. In fact, these satellite peaks appearing in our calculations for periodically distorted lattices are nothing but Bragg peaks, and the reason they appear at incommensurate positions in the previous figures is because of the naive (and intentional) way in which the unit cell for

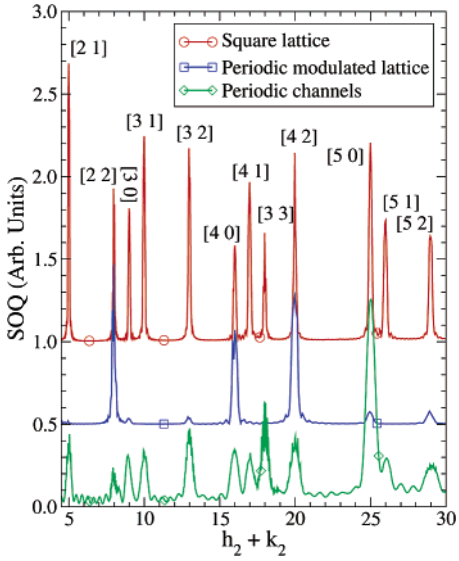

Figure 13. Structure factors for the square lattice, the periodic modulated lattice, and the lattice with periodic tetragonal channels. In this figure, the normalization factors for the different lattices are different, as we are only interested in the positions of the peaks of the distorted lattices compared with the positions of the Bragg reflections of the square lattice.

those lattices was chosen. To see this, let us consider two representative examples, namely, the periodically modulated lattice (Figure 4a) and the lattice with periodic channels of tetragonal distortions (Figure 6a). For the modulated lattice, it is easy to see that the resulting distorted lattice can be described as another square lattice in which the smallest motif that generates the whole lattice is another square unit cell of lattice parameter $2a$ with a basis of 4 atoms. For the channel of tetragonal distortions, the elementary motif is another square lattice of lattice parameter $7a$ with a basis of 58 atoms. If we now use the correct values for the size of the unit cell, we will obtain results as the ones depicted in Figure 13. As we can see, what seemed to be satellite peaks at incommensurate positions in h and k are nothing but Bragg reflections occurring at the same positions as the ones of the square lattice. Of course, the relations between the intensities of these peaks are completely different from the ones for the simple square lattice, because of the relative positions of the atoms inside the unit cell. Actually, these geometrical relations lead in some cases to a cancellation of the intensity of some peaks, what is usually called an extinction of the peak. This is especially noticeable in these

examples for the modulated lattice, in which all of the peaks with both *h* and *k* odd are absent, those with mixed *h* and *k* are almost extinct, and the relative intensities of the peaks with both *h* and *k* even are unaffected. The analysis for the lattice with periodic channels of tetragonal distortions is more complicated. To begin with, the original 40 × 40 lattice considered in this work contains only 5 × 5 periodic unit cells. Thus, the shapes and intensities of the peaks at very low Q are extremely affected by the finite size of the lattice, and the intensities of these peaks are of the same order of magnitude as the oscillatory tails of the Bragg peaks (which are also associated to the finite size of the lattices), making it very difficult to distinguish among them. For this reason, we repeated the calculation for a bigger lattice containing 13 × 13 unit cells (which amounts to 9802 atoms) and reduced the interatomic distance of the undistorted lattice to 1 Å. In doing so, the Bragg peaks are easily distinguished from the oscillatory tails. The result of this calculation shows again that the satellite peaks of Figure 12b are nothing but Bragg peaks when a truly periodic unit cell is chosen. Furthermore, all of the reflections are present in this case. The main effect of the complicated basis is that the intensity ratios of the reflections are completely different from the corresponding ones for the square lattice.

Obviously, we have not said anything new in this subsection, as all these facts have been known for a long time.[33] However, we think it is worthy to stress this point, as it seems that other authors at times forget to mention these elementary facts when analyzing diffraction patterns of lattices with periodic distortions.

B. A Comment on the Importance of the Lattice Size. As stated above, the present calculations have been carried out for relatively small lattices so the computation time is small enough. The reason the calculation of the SF takes so long is that the CRYGEN2D code does not make any attempt to use symmetry operations to reduce the number of operations in evaluating expression 3. In this way, it possible to calculate the SF for aperiodic lattices. For example, the CPU time for the lattices considered in this work is of the order of 24 h in a very fast computer (Compaq Alpha EV67 dual processor machine). Of course, the finite size of the lattices could raise the question of whether the number of diffracting sites is enough as to make any statements about the diffuse part of the scattering in the calculated diffraction patterns. The answer is that even for these relatively small lattices the diffuse part of the calculated diffraction patterns is correct. There are two ways of assessing this. The first one was already pointed out at the beginning of this section. We have repeated the present calculations for larger versions of some of the lattices reported in this work. In particular, the maximum size used for such calculations was 128 × 128 (16384 sites). The result of this analysis is that the calculated $S(Q)$ are similar to the ones reported in this work. Of course, the Bragg peaks are somewhat narrower, but once properly normalized, the diffuse part of the scattering is exactly the same. Someone, however, could argue that these results cannot be extrapolated to the thermodynamic limit. For that reason, we used a second, more rigorous, test. Starting from the calculated SF for the 40 × 40 lattices, we reconstructed the RDF by making use of the well-known relation[34,35]

$$\mathrm{PDF}(r) = 1 + \frac{1}{2\pi n}\int_0^\infty [S(Q) - 1]J_0(Q)Q\,\mathrm{d}Q \qquad (5)$$

where PDF(r) is the pair distribution function (the RDF is easily obtained from this), n is the particle density, and $J_0(Q)$ is the zero-th order Bessel function. The advantage of this method resides on the fact that the RDF is an intensive quantity (as far as the maximum value of r does not exceed the side of the lattice). Therefore, if the correct RDF is obtained by Fourier transforming the SF, that means that all of the pair correlations are present in the diffuse part of the diffraction pattern. In Figure 14, we report the results of such a calculation for the $S(Q)$ of a perfect square lattice, and the periodic and aperiodic channels, which are excellent examples of the conclusions reached below. The square lattice is included mainly as a test of the merit of the calculated RDFs (as it does not contain any extra peaks corresponding to distortions). As can be seen from the observation of that figure, the reconstructed RDFs are practically indistinguishable from the exact ones. Therefore, it seems that 40 × 40 lattices are enough to calculate structure factors that contain all of the pair correlations. Similar results are reached

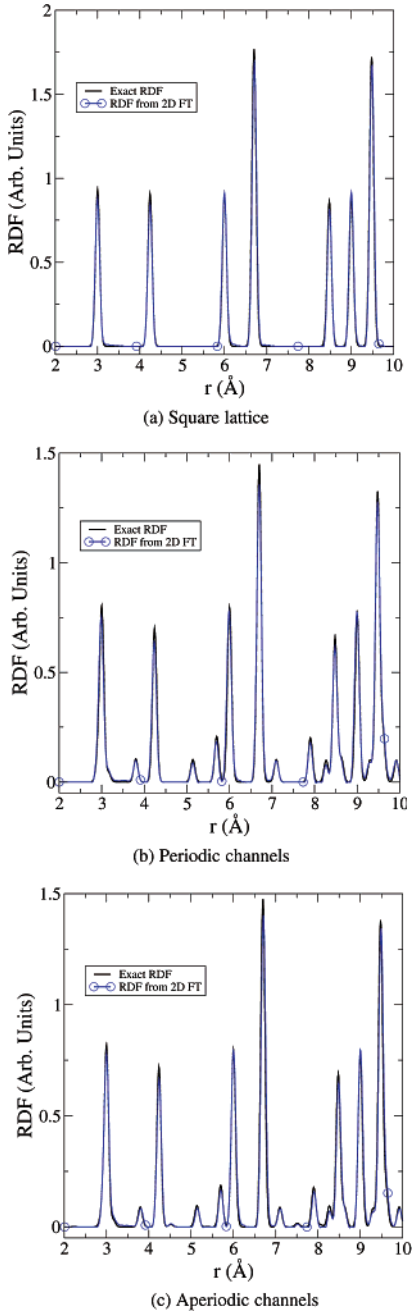

Figure 14. Exact and reconstructed RDFs for some of the lattices reported in this work. The exact RDF was calculated with the program CRYGEN, which calculates the average over the pair distances between the sites in the lattice. The curves labeled as "RDF from 2D FT" have been obtained from the pair distribution function calculated with (5).

for the rest of the lattices considered in this work, but we will not report them here.

IV. Conclusions

This work is concerned with the effects of certain types of static distortions, both periodic and aperiodic, local and collective, in the diffraction patterns of materials. Starting from a 2D square lattice, we have implemented different kinds of distortions to obtain new, periodic or aperiodic, 2D lattices. The radial distribution functions and structure factors for these lattices have been computed. The main result coming from the calculations is that periodic distortions are easily identified in the structure factors as new superlattice peaks or, equivalently, as extinction of certain Bragg reflections or changes in the relative intensities when the correct unit cell is chosen, as is known. When the periodicity of the distortions is lost, there are also some signatures present in the $S(Q)$, for example, an enhanced and asymmetric diffuse background around the fundamental peaks of the original lattice or oscillations of this same background. However, it is very difficult, if not impossible, to assess the exact nature of these distortions (i.e., whether they are vacancies or random displacements, for example). This fact is nothing but the realization, for the particular examples presented in this work, of the aforementioned uniqueness problem in the determination of the real structure of a material taking as a starting point the diffraction pattern.

It is important to stress at this point that the experimental situation can be even more misleading than the results presented in this work, as experimental measurements are always subject to additional effects we have not taken into account in our simulations. These include limited Q resolution, instrumental broadening, and noise. Instrumental broadening, especially, can very easily mask some of the peak splittings we obtain in our calculations. Regarding the calculated radial distribution functions, in some cases we have seen that they provide more intuitive information than the $S(Q)$ for the kinds of distortions considered in this work. This fact strongly supports the idea that PDF measurements can be crucially important in making progress in the problem of the determination of the structure of complex systems. However, this approach is not exempt to limitations. On one hand, it is necessary to use very intense sources in order to be able to measure the diffraction pattern up to very large values of Q ($\sim 35-45$ Å^{-1} typically). Fortunately, with the availability of very intense synchrotron and neutron sources, this problem is partially alleviated, and these wave vectors are experimentally achievable. On the other hand, the main limitation in extracting information from experimentally (Fourier transformed diffraction data) determined pair distribution functions is the effect of thermal broadening that can very easily mask some of the features associated to local distortions. We have seen some examples of this problem when studying the effects of small domains with tetragonal distortions in the radial distribution function: the new peaks associated with the new, shorter distances of the tetragonal phase are closer to the peaks associated to the pair distances of the square lattice than the width of those peaks, making it very difficult to distinguish them. What is even worse, the radial distribution function is completely oblivious to certain kinds of distortions (as it happened with the vacancies configurations). It is in these situations where X-ray absorption fine structure could play an important role, as this type of probe is sensitive to local distortions and to the different species present in the sample. The main limitation in this case is associated to the fact that the XAFS spectra contain multiple scattering contributions, and thus, the kinematic limit is not applicable to the analysis of the data, making it extremely difficult to extract information about the radial distribution at long distances from the probed atom.

We also want to emphasize that, obviously, we are aware of the fact that the kind of distortions we have studied in this work hardly exist in real materials. They are simple illustrative examples of how easy it is to miss important structural information about local and collective distortions if we blindly trust structural models obtained by only applying conventional diffraction analysis methods. Our intention is to motivate awareness about this potential problem. The emerging picture of complex solids strongly supports the idea that local and nanoscale distortions exist (probably even more complicated ones than the toy models we have studied in this work), there are mechanisms that make them stable, and they play an important role in the properties of these systems. However, as has been shown throughout this work, the signatures of such aperiodic distortions are subtle and misleading interpretations can be reached if special care is not paid to their analysis.

We think that the above paragraphs serve to further stress the point already made in the Introduction: It is necessary to use a combination of experimental methods that probe all of the relevant length scales (X-ray and neutron diffraction experiments, XAFS, PDF, etc.). At the same time, a combination of structural analysis methods (PDF analysis, reverse Monte Carlo simulations, etc.), beyond the standard Rietveld analysis, is necessary in order to reach a consistent picture of the structure of complex solids that can lead us to understand and exploit their properties.

Acknowledgment. This work was supported by DOE DP and OBES Division of Chemical Sciences under Contract W-7405. We want to thank T. Egami, A. Lawson, and Th. Proffen for very helpful discussions.

References and Notes

(1) Welberry, T. R.; Butler, B. D. *Chem. Rev.* **1995**, *95*, 2369.
(2) Warren, B. E. *X-ray Diffraction*; Dover: New York, 1990.
(3) Conradson, S. D. *Appl. Spectrosc.* **1998**, *52*, A252.
(4) Proceedings of the *Local and Nanoscale Structure in Complex Systems 2002* conference. Conradson, S. D., Ed.; to be published in *Journal of Nanoscience and Nanotechnology*.
(5) Ice, G. E.; Sparks, C. J. *Annu. Rev. Mater. Sci.* **1999**, *29*, 25.
(6) Xu, Z. A.; Ong, N. P.; Wang, Y.; Kakeshita, T.; Uchida, S. *Nature* **2000**, *406*, 486.
(7) Zaanen, J. *Nature* **2000**, *404*, 714.
(8) Moreo, A.; Yunoki, S.; Dagotto, E. *Science* **1999**, *283*, 2034.
(9) Dagotto, E.; Hotta, T.; Moreo, A. *Phys. Rep.* **2001**, *344*, 1.
(10) Tranquada, J. M.; Sternlieb, B. J.; Axe, J. D.; Nakamura, Y.; Uchida, S. *Nature* **1995**, *375*, 561.
(11) Tranquada, J. M.; Nakajima, K.; Braden, M.; Pintschovius, L.; McQueeney, R. J. *Phys. Rev. Lett.* **2002**, *88*, 075505.
(12) Welberry, T. R.; Butler, B. D. *J. Appl. Crystallogr.* **1994**, *27*, 205.
(13) Welberry, T. R.; Proffen, Th.; Bown, M. *Acta Crystallogr.* **1998**, *A54*, 661.
(14) Welberry, T. R. *Acta Crystallogr.* **2001**, *A54*, 244.
(15) Tomy, Bh.; Egami, T. *Acta Crystallogr.* **1992**, *A48*, 336.
(16) Proffen, Th.; Petkov, V.; Billinge, S. J. L.; Vogt, T. *Z. Kristallogr.* **2002**, *217*, 47.
(17) Proffen, Th. *Z. Kristallogr.* **2000**, *215*, 661.
(18) Bianconi, A.; Saini, N. L.; Lanzara, A.; Missori, M.; Rossetti, T.; Oyanagi, H.; Yamaguchi, H.; Oka, K.; Ito, T. *Phys. Rev. Lett.* **1996**, *76*, 3412.
(19) Saini, N. L.; Oyanagi, H.; Lanzara, A.; Di Castro, D.; Agrestini, S.; Bianconi, A.; Nakamura, F.; Fujita, T. *Phys. Rev. B* **2001**, *64*, 132510.
(20) Bianconi, A. *Int. J. Mod. Phys. B* **2000**, *14*, 3289.
(21) Villella, P.; Conradson, S. D.; Espinosa-Faller, F. J.; Foltyn, S. R.; Sickafus, K. E.; Valdez, J. A.; Degueldre, C. A. *Phys. Rev. B* **2001**, *64*, 104101.

(22) Espinosa, F. J.; Villella, P.; Lashley, J. C.; Conradson, S. D.; Cox, L. E.; Martinez, R.; Martinez, B.; Morales, L.; Terry, J.; Pereyra, R. A. *Phys. Rev. B* **2001**, *63*, 174111.

(23) Espinosa, F. J.; de Leon, J. M.; Conradson, S. D.; Pea, J. L.; Zapata-Torres, M. *Phys. Rev. B* **2000**, *61*, 7428.

(24) Tyson, T. A.; de Leon, J. M.; Conradson, S. D.; Bishop, A. R.; Neumeier, J. J.; Rder, H.; Zang, J. *Phys. Rev. B* **1996**, *53*, 13985−13988.

(25) Li, G. G.; Bridges, F.; Boyce, J. B.; Claeson, T.; Strom, C.; Eriksson, S.-G.; Conradson, S. D. *Phys. Rev. B* **1995**, *51*, 8564.

(26) Cox, L. E.; Martinez, R.; Nickel, J. H.; Conradson, S. D.; Allen, P. G. *Phys. Rev. B* **1995**, *51*, 751−755.

(27) Li, G. G.; Mustre de Leon, J.; Conradson, S. D.; Lovato, M. V.; Subramanian, M. A. *Phys. Rev. B* **1994**, *50*, 3356−3362.

(28) Dmowski, W.; McQueeney, R. J.; Egami, T.; Feng, Y. P.; Sinha, S. K.; Hinatsu, T.; Uchida, S. *Phys. Rev. B* **1995**, *52*, 6829.

(29) Vasiliu-Doloc, L.; Rosenkranz, S.; Osborn, R.; Sinha, S. K.; Lynn, J. W.; Mesot, J.; Seeck, O. H.; Preosti, G.; Fedro, A. J.; Mitchell, J. F. *Phys. Rev. Lett.* **1999**, *83*, 4393.

(30) Shimomura, S.; Wakabayashi, N.; Kuwahara, H.; Tokura, Y. *Phys. Rev. Lett.* **1999**, *83*, 4389.

(31) Villella, P.; Dimitrov, D.; Conradson, S. D. unpublished. Villela, P. Ph.D. Thesis unpublished

(32) Chung, J. S.; Thorpe, M. F. *Phys. Rev. B* **1999**, *59*, 4807.

(33) Ashcroft, N. W.; Mermin, N. D. *Solid State Physics*; Saunders: Philadelphia, 1976.

(34) Dimitrov, D. A.; Bishop, A. R.; Conradson, S. D. *Phys. Rev. B* **1997**, *56*, 2969.

(35) Thorpe, M. F.; Levashov, V. A.; Lei, M.; Billingue, S. J. L. In *From semiconductors to proteins: beyond the average structure*; Billingue, S. J. L., Thorpe, M. F., Eds.; Kluwer Academic/Plenum Publishers: New York, 2002; pp 105−128.

(36) In fact, one can expect the situation to be even more misleading in three-dimensions, as there are many more possible types of collective distortions.

(37) And the lattice is not truly periodic. It is interesting to notice that the $S(Q)$ does not reflect this fact.